

On the Potential Galactic Origin of the Ultra-High-Energy Event KM3-230213A

O. ADRIANI,^{1,2} S. AIELLO,³ A. ALBERT,^{4,5} A. R. ALHEBSI,⁶ M. ALSHAMSÍ,⁷ S. ALVES GARRE,⁸ A. AMBROSONE,^{9,10}
F. AMELI,¹¹ M. ANDRE,¹² L. APHECETCHE,¹³ M. ARDID ,¹⁴ S. ARDID,¹⁴ J. AUBLIN,¹⁵ F. BADARACCO,^{16,17}
L. BAILLY-SALINS,¹⁸ Z. BARDAČOVÁ,^{19,20} B. BARET,¹⁵ A. BARIEGO-QUINTANA,⁸ Y. BECHERINI,¹⁵ M. BENDAHMAN,¹⁰
F. BENFENATI GUALANDI,^{21,22} M. BENHASSI,^{23,10} M. BENNANI,¹⁸ D. M. BENOIT,²⁴ E. BERBEE,²⁵ E. BERTI,¹ V. BERTIN,⁷
P. BETTI,¹ S. BIAGI,²⁶ M. BOETTCHER,²⁷ D. BONANNO,²⁶ S. BOTTALÍ,¹ A. B. BOUASLA,²⁸ J. BOUMAAZA,²⁹ M. BOUTA,⁷
M. BOUWHUIS,²⁵ C. BOZZA,^{30,10} R. M. BOZZA,^{9,10} H. BRÂNZAŞ,³¹ F. BRETAUDEAU,¹³ M. BREUHAUS ,⁷ R. BRUIJN,^{32,25}
J. BRUNNER,⁷ R. BRUNO,³ E. BUIS,^{33,25} R. BUOMPANE,^{23,10} J. BUSTO,⁷ B. CAIFFI,¹⁶ D. CALVO,⁸ A. CAPONE,^{11,34}
F. CARENINI,^{21,22} V. CARRETERO,^{32,25} T. CARTRAUD,¹⁵ P. CASTALDI,^{35,22} V. CECCHINI,⁸ S. CELLI,^{11,34} L. CERISY,⁷
M. CHABAB,³⁶ A. CHEN,³⁷ S. CHERUBINI,^{38,26} T. CHIARUSI,²² M. CIRCELLA,³⁹ R. CLARK,⁴⁰ R. COCIMANO,²⁶
J. A. B. COELHO,¹⁵ A. COLEIRO,¹⁵ A. CONDORELLI,¹⁵ R. CONIGLIONE,²⁶ P. COYLE,⁷ A. CREUSOT,¹⁵ G. CUTTONE,²⁶
R. DALLIER,¹³ A. DE BENEDITTIS,¹⁰ G. DE WASSEIGE,⁴⁰ V. DECOENE,¹³ P. DEGUIRE,⁷ I. DEL ROSSO,^{21,22}
L. S. DI MAURO,²⁶ I. DI PALMA,^{11,34} A. F. DÍAZ,⁴¹ D. DIEGO-TORTOSA,²⁶ C. DISTEFANO,²⁶ A. DOMI,⁴² C. DONZAUD,¹⁵
D. DORNIC,⁷ E. DRAKOPOULOU,⁴³ D. DROUHIN,^{4,5} J.-G. DUCOIN,⁷ P. DUVERNE,¹⁵ R. DVORNICKÝ,¹⁹ T. EBERL,⁴²
E. ECKEROVÁ,^{19,20} A. EDDYMAOUI,²⁹ T. VAN EEDEN,²⁵ M. EFF,¹⁵ D. VAN ELJK,²⁵ I. EL BOJADDAINI,⁴⁴ S. EL HEDRI,¹⁵
S. EL MENTAWI,⁷ V. ELLAJOSYULA,^{16,17} A. ENZENHÖFER,⁷ G. FERRARA,^{38,26} M. D. FILIPOVIĆ,⁴⁵ F. FILIPPINI,²²
D. FRANCIOTTI,²⁶ L. A. FUSCO,^{30,10} T. GAL,⁴² J. GARCÍA MÉNDEZ,¹⁴ A. GARCIA SOTO,⁸ C. GATIUS OLIVER,²⁵
N. GEISSELBRECHT,⁴² E. GENTON,⁴⁰ H. GHADDARI,⁴⁴ L. GIALANELLA,^{23,10} B. K. GIBSON,²⁴ E. GIORGIO,²⁶ I. GOOS,¹⁵
P. GOSWAMI,¹⁵ S. R. GOZZINI,⁸ R. GRACIA,⁴² C. GUIDI,^{17,16} B. GUILLON ,¹⁸ M. GUTIÉRREZ,⁴⁶ C. HAACK,⁴²
H. VAN HAREN,⁴⁷ A. HEIJBOER,²⁵ L. HENNIG,⁴² J. J. HERNÁNDEZ-REY ,⁸ A. IDRISSE,²⁶ W. IDRISSE IBNSALIH,¹⁰
G. ILLUMINATI,²² O. JANIK,⁴² D. JOLY,⁷ M. DE JONG,^{48,25} P. DE JONG,^{32,25} B. J. JUNG,²⁵ P. KALACZYŃSKI,^{49,50}
J. KEEGANS,²⁴ V. KIKVADZE,⁵¹ G. KISTAURI,^{52,51} C. KOPPER,⁴² A. KOUCHNER,^{53,15} Y. Y. KOVALEV,⁵⁴ L. KRUPA,²⁰
V. KUEVIKOE,²⁵ V. KULIKOVSKIY,¹⁶ R. KVATADZE,⁵² M. LABALME,¹⁸ R. LAHMANN,⁴² M. LAMOUREUX,⁴⁰ G. LAROSA,²⁶
C. LASTORIA,¹⁸ J. LAZAR,⁴⁰ A. LAZO,⁸ S. LE STUM,⁷ G. LEHAUT,¹⁸ V. LEMAÎTRE,⁴⁰ E. LEONORA,³ N. LESSING,⁸
G. LEVI,^{21,22} M. LINDSEY CLARK,¹⁵ F. LONGHITANO,³ F. MAGNANI,⁷ J. MAJUMDAR,²⁵ L. MALERBA,^{16,17} F. MAMEDOV,²⁰
A. MANFREDA,¹⁰ A. MANOUSAKIS,⁵⁵ M. MARCONI,^{17,16} A. MARGIOTTA,^{21,22} A. MARINELLI,^{9,10} C. MARKOU,⁴³ L. MARTIN,¹³
M. MASTRODICASA,^{34,11} S. MASTROIANNI,¹⁰ J. MAURO,⁴⁰ K. C. K. MEHTA,⁵⁰ A. MESKAR,⁵⁶ G. MIELE,^{9,10} P. MIGLIOZZI,¹⁰
E. MIGNECO,²⁶ M. L. MITSOU,^{23,10} C. M. MOLLO,¹⁰ L. MORALES-GALLEGOS ,^{23,10} N. MORI ,¹ A. MOUSSA,⁴⁴
I. MOZUN MATEO,¹⁸ R. MULLER,²² M. R. MUSONE,^{23,10} M. MUSUMECI,²⁶ S. NAVAS ,⁴⁶ A. NAYERHODA,³⁹
C. A. NICOLAU,¹¹ B. NKOSI,³⁷ B. Ó FEARRAIGH ,¹⁶ V. OLIVIERO,^{9,10} A. ORLANDO,²⁶ E. OUKACHA,¹⁵ L. PACINI,¹
D. PAESANI,²⁶ J. PALACIOS GONZÁLEZ,⁸ G. PAPALASHVILI,^{39,51} P. PAPINI,¹ V. PARISI,^{17,16} A. PARMAR,¹⁸
E. J. PASTOR GÓMEZ,⁸ C. PASTORE,³⁹ A. M. PÄUN,³¹ G. E. PÁVĽAŠ,³¹ S. PEÑA MARTÍNEZ,¹⁵ M. PERRIN-TERRIN,⁷
V. PESTEL,¹⁸ R. PESTES,¹⁵ M. PETROPAVLOVA,^{20,57} P. PIATTELLI,²⁶ A. PLAVIN,^{54,58} C. POIRÈ,^{30,10} V. POPA,^{31,*}
T. PRADIER,⁴ J. PRADO,⁸ S. PULVIRENTI,²⁶ C. A. QUIROZ-RANGEL,¹⁴ N. RANDAZZO,³ A. RATNANI,⁵⁹ S. RAZZAQUE,⁶⁰
I. C. REA,¹⁰ D. REAL,⁸ G. RICCOBENE,²⁶ J. ROBINSON,²⁷ A. ROMANOV,^{17,16,18} E. ROS,⁵⁴ A. ŠAINA,⁸ F. SALESA GREUS,⁸
D. F. E. SAMTLEBEN,^{48,25} A. SÁNCHEZ LOSA,⁸ S. SANFILIPPO ,²⁶ M. SANGUINETI,^{17,16} D. SANTONOCITO,²⁶ P. SAPIENZA,²⁶
M. SCARINGELLA,¹ M. SCARNERA,^{40,15} J. SCHNABEL,⁴² J. SCHUMANN,⁴² H. M. SCHUTTE,²⁷ J. SENECA,²⁵ N. SENNAN,⁴⁴
P. A. SEVLE MYHR,⁴⁰ I. SGURA,³⁹ R. SHANIDZE,⁵¹ A. SHARMA,¹⁵ Y. SHITOV,²⁰ F. ŠIMKOVIC,¹⁹ A. SIMONELLI,¹⁰
A. SINOPOULOU,³ B. SPISSO,¹⁰ M. SPURIO,^{21,22} O. STARODUBTSEV,¹ D. STAVROPOULOS,⁴³ I. ŠTEKL,²⁰ D. STOCCO,¹³
M. TAIUTI,^{17,16} G. TAKADZE,⁵¹ Y. TAYALATI,^{29,59} H. THIERSEN,²⁷ S. THODAM,⁶ I. TOSTA E MELO,^{3,38} B. TROCMÉ,¹⁵
V. TSOURAPIS,⁴³ E. TZAMARIUDAKI,⁴³ A. UKLEJA,^{56,50} A. VACHERET,¹⁸ V. VALSECCHI,²⁶ V. VAN ELEWYCK,^{53,15}
G. VANNOYE,^{7,16,17} E. VANNUCCINI,¹ G. VASILEIADIS,⁶¹ F. VAZQUEZ DE SOLA,²⁵ A. VEUTRO,^{11,34} S. VIOLA,²⁶
D. VIVOLO,^{23,10} A. VAN VLIET,⁶ E. DE WOLF,^{32,25} I. LHENRY-YVON,¹⁵ S. ZAVATARELLI,¹⁶ A. ZEGARELLI,^{11,34} D. ZITO,²⁶
J. D. ZORNOZA,⁸ J. ZÚÑIGA,⁸ AND N. ZYWUCKA²⁷

¹INFN, Sezione di Firenze, via Sansone 1, Sesto Fiorentino, 50019 Italy

²Università di Firenze, Dipartimento di Fisica e Astronomia, via Sansone 1, Sesto Fiorentino, 50019 Italy

³INFN, Sezione di Catania, (INFN-CT) Via Santa Sofia 64, Catania, 95123 Italy

⁴Université de Strasbourg, CNRS, IPHC UMR 7178, F-67000 Strasbourg, France

⁵Université de Haute Alsace, rue des Frères Lumière, 68093 Mulhouse Cedex, France

⁶Khalifa University of Science and Technology, Department of Physics, PO Box 127788, Abu Dhabi, United Arab Emirates

- ⁷ Aix Marseille Univ, CNRS/IN2P3, CPPM, Marseille, France
- ⁸ IFIC - Instituto de Física Corpuscular (CSIC - Universitat de València), c/Catedrático José Beltrán, 2, 46980 Paterna, Valencia, Spain
- ⁹ Università di Napoli “Federico II”, Dip. Scienze Fisiche “E. Pancini”, Complesso Universitario di Monte S. Angelo, Via Cintia ed. G, Napoli, 80126 Italy
- ¹⁰ INFN, Sezione di Napoli, Complesso Universitario di Monte S. Angelo, Via Cintia ed. G, Napoli, 80126 Italy
- ¹¹ INFN, Sezione di Roma, Piazzale Aldo Moro 2, Roma, 00185 Italy
- ¹² Universitat Politècnica de Catalunya, Laboratori d'Aplicacions Bioacústiques, Centre Tecnològic de Vilanova i la Geltrú, Avda. Rambla Exposició, s/n, Vilanova i la Geltrú, 08800 Spain
- ¹³ Subatech, IMT Atlantique, IN2P3-CNRS, Nantes Université, 4 rue Alfred Kastler - La Chantrerie, Nantes, BP 20722 44307 France
- ¹⁴ Universitat Politècnica de València, Instituto de Investigación para la Gestión Integrada de las Zonas Costeras, C/ Paranimf, 1, Gandia, 46730 Spain
- ¹⁵ Université Paris Cité, CNRS, Astroparticule et Cosmologie, F-75013 Paris, France
- ¹⁶ INFN, Sezione di Genova, Via Dodecaneso 33, Genova, 16146 Italy
- ¹⁷ Università di Genova, Via Dodecaneso 33, Genova, 16146 Italy
- ¹⁸ LPC CAEN, Normandie Univ, ENSICAEN, UNICAEN, CNRS/IN2P3, 6 boulevard Maréchal Juin, Caen, 14050 France
- ¹⁹ Comenius University in Bratislava, Department of Nuclear Physics and Biophysics, Mlynska dolina F1, Bratislava, 842 48 Slovak Republic
- ²⁰ Czech Technical University in Prague, Institute of Experimental and Applied Physics, Husova 240/5, Prague, 110 00 Czech Republic
- ²¹ Università di Bologna, Dipartimento di Fisica e Astronomia, v.le C. Berti-Pichat, 6/2, Bologna, 40127 Italy
- ²² INFN, Sezione di Bologna, v.le C. Berti-Pichat, 6/2, Bologna, 40127 Italy
- ²³ Università degli Studi della Campania “Luigi Vanvitelli”, Dipartimento di Matematica e Fisica, viale Lincoln 5, Caserta, 81100 Italy
- ²⁴ E. A. Milne Centre for Astrophysics, University of Hull, Hull, HU6 7RX, United Kingdom
- ²⁵ Nikhef, National Institute for Subatomic Physics, PO Box 41882, Amsterdam, 1009 DB Netherlands
- ²⁶ INFN, Laboratori Nazionali del Sud, (LNS) Via S. Sofia 62, Catania, 95123 Italy
- ²⁷ North-West University, Centre for Space Research, Private Bag X6001, Potchefstroom, 2520 South Africa
- ²⁸ Université Badji Mokhtar, Département de Physique, Faculté des Sciences, Laboratoire de Physique des Rayonnements, B. P. 12, Annaba, 23000 Algeria
- ²⁹ University Mohammed V in Rabat, Faculty of Sciences, 4 av. Ibn Battouta, B.P. 1014, R.P. 10000 Rabat, Morocco
- ³⁰ Università di Salerno e INFN Gruppo Collegato di Salerno, Dipartimento di Fisica, Via Giovanni Paolo II 132, Fisciano, 84084 Italy
- ³¹ ISS, Atomistilor 409, Măgurele, RO-077125 Romania
- ³² University of Amsterdam, Institute of Physics/IHEF, PO Box 94216, Amsterdam, 1090 GE Netherlands
- ³³ TNO, Technical Sciences, PO Box 155, Delft, 2600 AD Netherlands
- ³⁴ Università La Sapienza, Dipartimento di Fisica, Piazzale Aldo Moro 2, Roma, 00185 Italy
- ³⁵ Università di Bologna, Dipartimento di Ingegneria dell'Energia Elettrica e dell'Informazione “Guglielmo Marconi”, Via dell'Università 50, Cesena, 47521 Italia
- ³⁶ Cadi Ayyad University, Physics Department, Faculty of Science Semlalia, Av. My Abdellah, P.O.B. 2390, Marrakech, 40000 Morocco
- ³⁷ University of the Witwatersrand, School of Physics, Private Bag 3, Johannesburg, Wits 2050 South Africa
- ³⁸ Università di Catania, Dipartimento di Fisica e Astronomia “Ettore Majorana”, (INFN-CT) Via Santa Sofia 64, Catania, 95123 Italy
- ³⁹ INFN, Sezione di Bari, via Orabona, 4, Bari, 70125 Italy
- ⁴⁰ UCLouvain, Centre for Cosmology, Particle Physics and Phenomenology, Chemin du Cyclotron, 2, Louvain-la-Neuve, 1348 Belgium
- ⁴¹ University of Granada, Department of Computer Engineering, Automation and Robotics / CITIC, 18071 Granada, Spain
- ⁴² Friedrich-Alexander-Universität Erlangen-Nürnberg (FAU), Erlangen Centre for Astroparticle Physics, Nikolaus-Fiebiger-Straße 2, 91058 Erlangen, Germany
- ⁴³ NCSR Demokritos, Institute of Nuclear and Particle Physics, Ag. Paraskevi Attikis, Athens, 15310 Greece
- ⁴⁴ University Mohammed I, Faculty of Sciences, BV Mohammed VI, B.P. 717, R.P. 60000 Oujda, Morocco
- ⁴⁵ Western Sydney University, School of Computing, Engineering and Mathematics, Locked Bag 1797, Penrith, NSW 2751 Australia
- ⁴⁶ University of Granada, Dpto. de Física Teórica y del Cosmos & C.A.F.P.E., 18071 Granada, Spain
- ⁴⁷ NIOZ (Royal Netherlands Institute for Sea Research), PO Box 59, Den Burg, Texel, 1790 AB, the Netherlands
- ⁴⁸ Leiden University, Leiden Institute of Physics, PO Box 9504, Leiden, 2300 RA Netherlands
- ⁴⁹ AstroCeNT, Nicolaus Copernicus Astronomical Center, Polish Academy of Sciences, Rektorska 4, Warsaw, 00-614 Poland
- ⁵⁰ AGH University of Krakow, Al. Mickiewicza 30, 30-059 Krakow, Poland
- ⁵¹ Tbilisi State University, Department of Physics, 3, Chavchavadze Ave., Tbilisi, 0179 Georgia
- ⁵² The University of Georgia, Institute of Physics, Kostava str. 77, Tbilisi, 0171 Georgia
- ⁵³ Institut Universitaire de France, 1 rue Descartes, Paris, 75005 France
- ⁵⁴ Max-Planck-Institut für Radioastronomie, Auf dem Hügel 69, 53121 Bonn, Germany
- ⁵⁵ University of Sharjah, Sharjah Academy for Astronomy, Space Sciences, and Technology, University Campus - POB 27272, Sharjah, - United Arab Emirates
- ⁵⁶ National Centre for Nuclear Research, 02-093 Warsaw, Poland

⁵⁷*Faculty of Mathematics and Physics, Charles University in Prague, Prague, Czech Republic*

⁵⁸*Harvard University, Black Hole Initiative, 20 Garden Street, Cambridge, MA 02138 USA*

⁵⁹*School of Applied and Engineering Physics, Mohammed VI Polytechnic University, Ben Guerir, 43150, Morocco*

⁶⁰*University of Johannesburg, Department Physics, PO Box 524, Auckland Park, 2006 South Africa*

⁶¹*Laboratoire Univers et Particules de Montpellier, Place Eugène Bataillon - CC 72, Montpellier Cédex 05, 34095 France*

ABSTRACT

The KM3NeT observatory detected the most energetic neutrino candidate ever observed, with an energy between 72 PeV and 2.6 EeV at the 90% confidence level. The observed neutrino is likely of cosmic origin. In this article, it is investigated if the neutrino could have been produced within the Milky Way. Considering the low fluxes of the Galactic diffuse emission at these energies, the lack of a nearby potential Galactic particle accelerator in the direction of the event and the difficulty to accelerate particles to such high energies in Galactic systems, we conclude that if the event is indeed cosmic, it is most likely of extragalactic origin.

Keywords: –

1. INTRODUCTION

Neutrinos are unique cosmic messengers, produced exclusively through hadronic interactions. They allow us to probe regions of the Universe that are otherwise inaccessible and to discern leptonic from hadronic processes, which is usually very difficult to achieve unambiguously with electromagnetic observations alone. These elusive particles have opened new avenues in high-energy astrophysics research. Neutrino detectors such as AMANDA, IceCube, ANTARES, and Baikal-GVD demonstrated the feasibility of neutrino telescopes and provided the first groundbreaking results in the last decade, such as the measurements of the astrophysical neutrino flux (IceCube Collaboration 2013; Aartsen et al. 2016; Abbasi et al. 2024; Albert et al. 2018, 2024; Allakhverdyan et al. 2023) or the detection of neutrinos from the Galactic Plane (IceCube Collaboration et al. 2023). Also, the first likely associations of neutrinos with single sources, such as the blazar TXS 0506+056 or the active galaxy NGC 1068, have been achieved (IceCube Collaboration et al. 2018, 2022).

The KM3NeT neutrino telescope has detected the event KM3-230213A on the 13th of February 2023 (Aiello et al. 2025a). The event has a median neutrino energy of 220 PeV, with a 90% confidence interval ranging from 72 PeV to 2.6 EeV. This makes KM3-230213A the most energetic neutrino candidate event observed so far. Furthermore, the expected flux of atmospheric neutrinos above 100 PeV in KM3NeT is $1 - 5 \times 10^{-5}$ events per year (Aiello et al. 2025a), indicating that this event was quite unlikely to be produced by cosmic rays (CRs) interacting in the Earth's atmosphere. This detection marks a significant milestone in neutrino astronomy.

The origin of the event is not clear. While it is with extremely high probability a cosmic event, many different classes of objects are expected to produce neutrinos, such as active galactic nuclei (AGN), supernova remnants (SNRs), star-forming regions, γ -ray bursts and others. Also, large-scale emission from the Galactic Plane, from cosmogenic neutrinos, or unresolved sources can contribute to the neutrino flux measured on Earth. However, only a few types of sources are expected to be able to accelerate particles to the required energies.

In this article, we explore the possibility that the event is of Galactic origin, i.e. produced in the Milky Way, where potential production sites are astrophysical accelerators, gas targets and cosmic-ray collisions giving rise to a diffuse Galactic component. The position of KM3-230213A was determined to be RA = 94.3° and Dec = -7.8° , with containment radii of $R(68\%) = 1.5^\circ$, and $R(99\%) = 3.0^\circ$. The corresponding Galactic coordinates are $l = 216.1^\circ$ and $b = -11.1^\circ$. Therefore, the event occurred far away from the Galactic Centre, and $\sim 11^\circ$ offset from the Galactic Plane. We first search for potential gas targets within the vicinity of the event in section 2, as a correlation with gas is expected in the hadronic collision neutrino production channel. We then discuss the expected neutrino fluxes from the Galactic diffuse emission (subsection 3.1) and further search for possible nearby particle accelerators (subsection 3.2). The investigation is followed by a search for potential γ -ray counterparts and a derivation of upper limits on Galactic

* Deceased

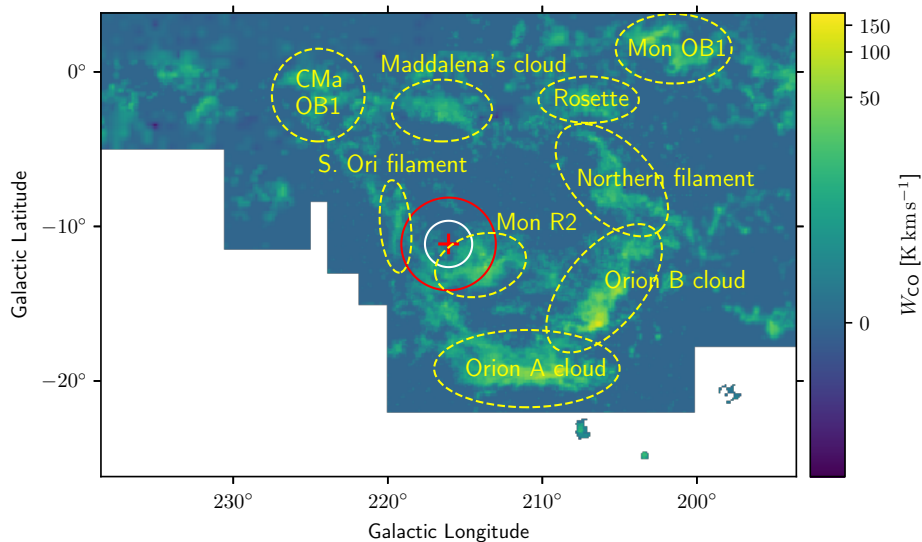


Figure 1. CO-map of the velocity integrated brightness temperature from Dame et al. (2001) with the KM3-230213A event superimposed: The cross marks the event position, and the white and red circles are the 68 % and 99 % containment radii, respectively. The dashed ellipses mark the location of molecular clouds in the region.

neutrino fluxes as a result of the non-detection of sources by the HAWC observatory (section 4). We conclude in section 5, where we summarize and discuss our results.

2. MOLECULAR GAS IN THE NEUTRINO EVENT VICINITY

In many environments in the Galaxy, the dominant hadronic production mechanism for neutrinos and γ -rays is the collision of CRs with other hadronic targets. To investigate whether there is an enhancement of molecular gas close to the KM3-230213A position, we used carbon monoxide (CO) emission maps from Dame et al. (2001). CO is a reliable tracer of molecular gas and is often used to estimate the total mass of molecular gas (e.g. Neining et al. 1998).

The CO map of the velocity integrated brightness temperature together with the KM3-230213A position and the 68 % and 99 % containment radii is shown in Figure 1. The different molecular clouds in the region are also indicated. These are: CMa OB1, Maddalena’s cloud, the Rosette molecular cloud, Monoceros OB1 (Mon OB1), the southern (S. Ori) and northern Orion filaments, Monoceros R2 (Mon R2), and the Orion A and Orion B clouds, with distances from the Earth between ~ 400 pc and ~ 2.4 kpc (Schlafly et al. 2014). As can be seen, no excess is observed directly at the KM3-230213A position. However, closely there are the S. Ori filament, and the Mon R2 cloud, the latter being in overlap with the 99 % containment radius of the neutrino event, thus it could be a potential target for CRs. Both the S. Ori filament and Mon R2 are relatively close to the Earth.

The S. Ori filament is estimated to be at a distance of ~ 900 pc and is potentially a ‘bridge’ between the Mon R2 and the CMa OB1 clouds (see Maddalena et al. 1986, and references therein). Its mass estimated from CO observations is $3 \times 10^4 M_{\odot}$, but estimates derived from the virial theorem or from the assumption of local thermodynamic equilibrium give larger values. It seems not to be a region of active star formation (Maddalena et al. 1986).

A commonly-adopted distance of Mon R2 from the Earth is (830 ± 50) pc (Racine 1968; Herbst & Racine 1976). It has a physical size of $44 \text{ pc} \times 88 \text{ pc}$ (Carpenter & Hodapp 2008) and a total mass of $\sim 9 \times 10^4 M_{\odot}$ (Maddalena et al. 1986). The molecular gas is not evenly distributed but exhibits a clumpy structure with a concentration towards the centre (e.g. Maddalena et al. 1986). Assuming a uniform distribution over a region of $44 \text{ pc} \times 88 \text{ pc} \times 44 \text{ pc}$, one obtains an average number density of $\sim 20 \text{ cm}^{-3}$. However, this estimate disregards the spatial shape of the cloud and from the CO maps one can infer that some fraction of the $44 \text{ pc} \times 88 \text{ pc}$ diameter does not contain mass. In the densest regions of the cloud, number densities are likely to reach several hundreds of particles per cm^3 . This is much larger

than the average Galactic interstellar medium density of $\sim 0.2 \text{ cm}^{-3}$ from the density model of [Ferrière \(1998\)](#); [Ferrière et al. \(2007\)](#) at the same location. In contrast to the S. Ori filament, Mon R2 is a site of ongoing star formation ([Jiang & Hillenbrand 2024](#)). Since the Mon R2 cloud overlaps with the 99% containment radius of KM3-230213A, in principle, it could serve as a target for neutrino production.

3. POTENTIAL COSMIC RAY SOURCES

A big challenge for a potential Galactic origin of KM3-230213A is its extreme energy. In the case of hadronic collisions, the interacting CR needs to have at least an energy of several hundreds of PeV, assuming the lower limit for the neutrino energy of 72 PeV. Thus it must be originating from sources contributing to the CR spectrum in the transition region between the “knee” and the “ankle” features. Many Galactic sources will fail to accelerate particles even to PeV energies. This is also reflected by the interpretation of the knee in the CR spectrum being caused by a rigidity-dependent cutoff of a Galactic source population ([Hörandel 2003](#)). The probability for this event being of Galactic origin is reduced even more taking into account the distance from the Galactic Centre and the offset of 11° from the Galactic Plane. In this section, we will explore potential CR sources, first for the case of the diffuse emission, and later for other known Galactic γ -ray sources.

3.1. Diffuse Galactic emission

The diffuse Galactic emission is produced by CRs propagating in the Milky Way and interacting with other nuclei in the Galaxy. The CR spectrum measured at Earth extends up to energies of several 10^{20} eV, although the most energetic CRs are expected to have extragalactic origin ([Abdul Halim et al. 2024](#)). Many different models for the Galactic diffuse emission were developed. These models differ, for example, in the considered CR composition, the diffusion properties of CRs in the Galaxy, and the distribution and injection of CRs from the sources. In particular, this modifies the subsequent CR distribution within the Galaxy in terms of total CR flux and potential spectral changes. Finally, these models use different γ -ray and CR datasets to obtain their estimates. The resulting γ -ray and neutrino emission is non-isotropic and follows the gas distribution of the Milky Way. We are specifically interested in the predicted emission at the location of KM3-230213A. To investigate how this localized flux compares to the overall emission, we use the model in [Breuhaus et al. \(2022\)](#) as an example case, as it was also focused on reproducing the γ -ray fluxes at hundreds of TeV, and compare the results later with predictions from the KRA_γ^5 model from [Gaggero et al. \(2015\)](#) and the newer KRA_γ min. and max. models from [De La Torre Luque et al. \(2022\)](#).

The model from [Breuhaus et al. \(2022\)](#) is tuned on γ -ray data from Tibet- AS_γ ([Amenomori et al. 2021](#)) and ARGO-YBJ ([Bartoli et al. 2015](#)) for Galactic longitudes $25^\circ \leq l \leq 100^\circ$ and Galactic latitudes with $|b| \leq 5^\circ$. Recently, the Galactic diffuse γ -ray emission was also observed by LHAASO ([Cao et al. 2023](#)), hence we additionally tuned the model to these data only. The models are compared to the all-sky diffuse flux of KM3-230213A.

The results are shown in [Figure 2](#) and [Figure 3](#), where a comparison of the following neutrino fluxes is presented: the all-sky diffuse KM3-230213A flux ([Aiello et al. 2025a](#)), measurements of neutrinos from the Galactic disk by IceCube for the π^0 and the KRA_γ^5 templates ([IceCube Collaboration et al. 2023](#)), and theoretical predictions for the cosmogenic neutrino flux and extragalactic sources taken from [Aiello et al. \(2025a\)](#). The neutrino fluxes at the position of KM3-230213A and the all-sky diffuse Galactic neutrino flux from Model A of [Breuhaus et al. \(2022\)](#) are shown in [Figure 2](#), tuned to data from Tibet- AS_γ and to measurements from LHAASO of the inner Galaxy region ($|b| < 5^\circ$, $15^\circ < l < 125^\circ$). We note that although the LHAASO region of the inner Galactic Plane overlaps with the one from Tibet AS_γ and ARGO-YBJ, it is not covering the same fraction of the sky. The model tuned on LHAASO data leads to lower predicted neutrino emission. This might be caused by the different source masking by Tibet AS_γ and LHAASO and it reflects uncertainties in the measurements of Galactic diffuse emission by current γ -ray observatories. As can be seen, at energies above several tens of PeV, the Galactic diffuse fluxes are well below the KM3-230213A flux as well as the bands of the cosmogenic neutrino flux and other extragalactic sources, making the association of KM3-230213A with a Galactic diffuse origin unlikely. Although the KM3-230213A flux is computed with the assumption of the emission being isotropic, which is not the case for the diffuse Galactic emission, using a non-isotropic template would not change the result significantly.

The exact composition of the CRs detected on Earth above PeV energies is not known and it can impact the resulting neutrino emission. To compare different emission scenarios, different compositional models from [Breuhaus et al. \(2022\)](#) are shown in [Figure 3](#). All of them are matched with the Tibet- AS_γ and ARGO-YBJ data, resulting in higher fluxes than when matching to data from LHAASO. To explore the maximum possible neutrino flux at higher energies, we

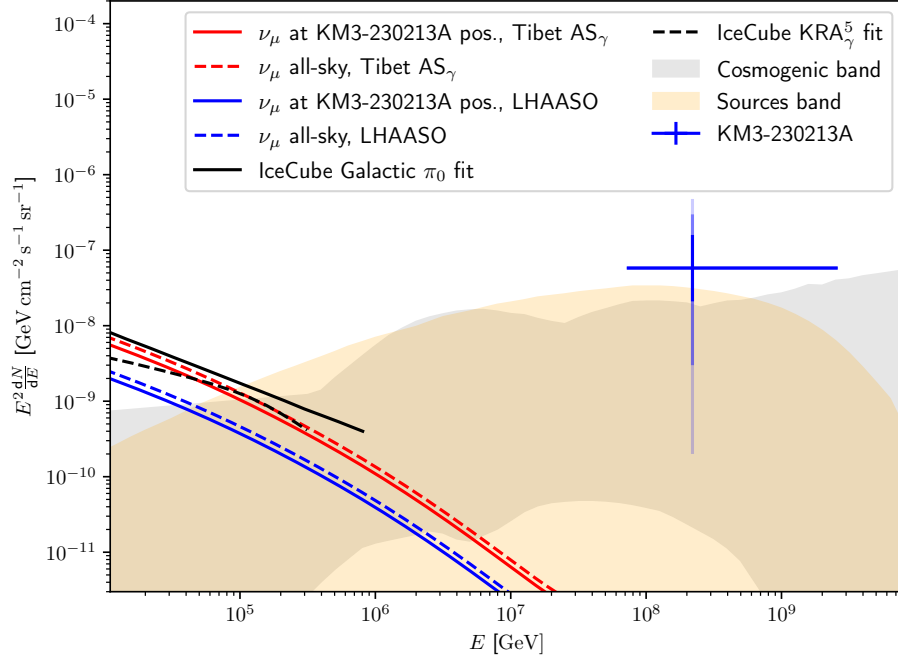


Figure 2. Expected neutrino fluxes from Model A of Breuhaus et al. (2022) compared to the flux derived from KM3-230213A (blue data point, the different blue shades represent the 1, 2 and 3 σ Feldman-Cousins confidence intervals, respectively, Aiello et al. (2025a)). Dashed colored lines represent the total angle-averaged Galactic neutrino fluxes and solid lines the flux at the position of KM3-230213A. Models tuned on Tibet-AS γ data are shown in red and the ones tuned on LHAASO data in blue. We also show measurements from IceCube of the Galactic diffuse neutrino flux for different models (black lines IceCube Collaboration et al. 2023) and the bands of the cosmogenic neutrino flux and individual extragalactic sources shown in Aiello et al. (2025a).

also show a case which was previously not in Breuhaus et al. (2022): the composition of the first Galactic component from Model A in Breuhaus et al. (2022) dominating below PeV energies is kept as in the original model. All other CR contributions are assumed to be hydrogen above PeV energies, matching the all-particle CR flux. Therefore, above the energies where we can not measure the individual CR composition directly with satellite observations, the CRs are assumed to have the lightest possible composition. This is, as in the pure hydrogen and the pure iron case, not expected to be a realistic situation but it produces the maximum possible neutrino fluxes above PeV energies. The lower energies, which are matched to the γ -ray data, still reproduce the direct CR measurements on Earth. Even in this case, the diffuse Galactic emission is not expected to dominate over the cosmogenic fluxes.

Other models of the diffuse Galactic emission as in Breuhaus et al. (2022) give similar results. To illustrate this, Figure 4 shows the range of all-sky neutrino fluxes from the models of Breuhaus et al. (2022), as well as the KRA γ^5 model from Gaggero et al. (2015) and the newer KRA γ min. and max. models from De La Torre Luque et al. (2022). Due to the steep spectral index of the diffuse CRs, the resulting fluxes above tens of PeV are negligible compared to other sources. Below PeV energies the atmospheric muon- and antimuon neutrino flux dominates over the average diffuse Galactic neutrino flux. Above \sim PeV energies, the diffuse Galactic emission is negligible compared to other expected neutrino fluxes, but it is still dominating over the atmospheric neutrinos (Aiello et al. 2025a).

By adopting a simple model for the Galactic density distribution at the location of KM3-230213A, such as the one from Ferrière (1998); Ferrière et al. (2007), the flux per steradian is reduced by $\sim 20\%$. This difference is smaller than changes caused by uncertainties in the CR models. The neutrino emission arising from dense target clouds, as Mon R2, is however expected to be enhanced. Estimations of the diffuse flux from Mon R2 were for example computed in Albert et al. (2021). Assuming that the emission is evenly distributed over an area of $14^\circ 2'$ (Maddalena et al. 1986), enhancements of around one order of magnitude are possible compared to Model A from Breuhaus et al. (2022). The material within Mon R2 is in fact not evenly spread out but rather concentrated in different clumpy regions (Carpenter & Hodapp 2008). This will produce regions with both lower and higher γ -ray fluxes compared

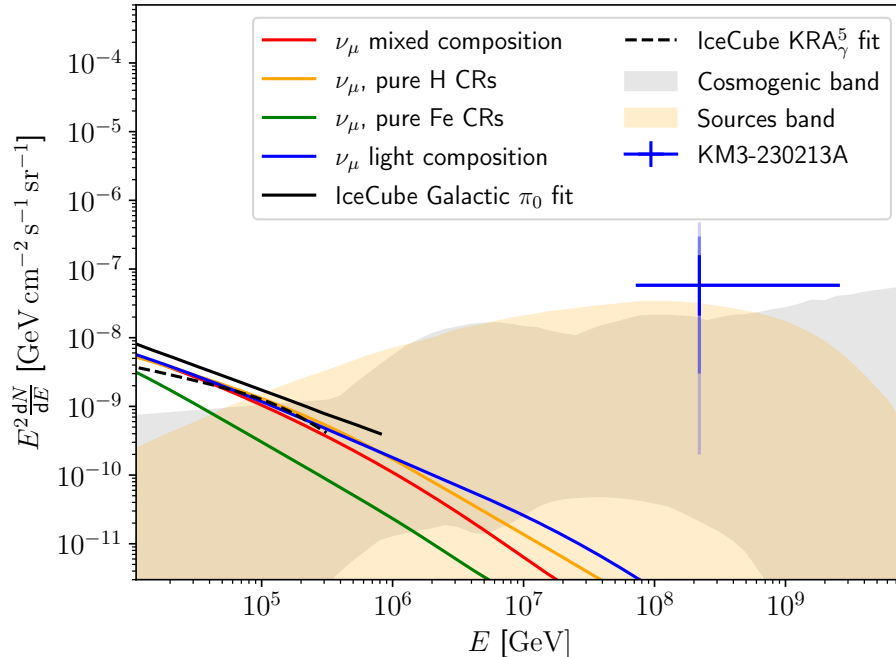


Figure 3. Expected neutrino fluxes from Models of Breuhaus et al. (2022) for different CR compositions compared to the flux derived from KM3-230213A (blue data point, the different blue shades represent the 1, 2 and 3 σ Feldman-Cousins confidence intervals, respectively, Aiello et al. (2025a)). Model A is shown in red, the pure hydrogen and pure iron cases are shown in orange and green, and the blue line is the model with mixed composition below PeV energies changing to a pure hydrogen spectrum above for maximum neutrino emission. IceCube measurements of the Galactic diffuse neutrino flux for different models (black lines IceCube Collaboration et al. 2023) and the bands of the cosmogenic neutrino flux and individual extragalactic sources from Aiello et al. (2025a) are also shown.

to computations assuming a homogeneous gas distribution. However, enhancements of many orders of magnitude, which would be needed for the diffuse Galactic neutrino flux to dominate over the cosmogenic neutrino flux or other extragalactic sources, are not possible. The diffuse Galactic neutrino flux is therefore negligible, both if it is produced in the diffuse interstellar medium and in the clouds investigated here.

3.2. Single sources

While the expected neutrino emission from the cloud Mon R2 caused by interactions of the diffuse Galactic CRs would not reproduce the flux inferred from the KM3-230213A measurement, the case in which a beam of accelerated particles from a nearby accelerator produces a larger emissivity can not be excluded. The challenge to explain the KM3-230213A neutrino with a single Galactic source comes from i) the presence of a possible accelerator, that can operate until the required energies, and ii) the gas target. A possible target for the neutrino event is the Mon R2 cloud (see section 2). An accelerator could also be located away from the emission site with its accelerated particles diffusing into Mon R2. However, if it is located too far away, the density of accelerated particles will be low. Additionally, if located at a similar distance to another cloud such as Orion A, the collisions with particles in this other cloud will also produce γ -rays and neutrinos. Depending on the gas densities, the emission from the second cloud can be comparable to or even higher than the emission from Mon R2. A source outside the Mon R2 cloud would produce γ -ray emission within the whole cloud and therefore Mon R2 should appear bright in γ -rays. Such a scenario is inconsistent with the non-detection of Mon R2 by HAWC (Albert et al. 2021, see subsection 4.1). An optically thick source in γ -rays which is bright in neutrino emission can therefore be only located inside Mon R2, with the neutrinos produced in a rather small region with strong radiation fields. In the following, different potential source types are investigated.

Supernova remnants (SNRs): Although SNRs might only be able to accelerate particles until PeV energies in their earliest phases shortly after the supernova explosions (Lagage & Cesarsky 1983; Bell et al. 2013; Marcowith et al. 2018), it was argued recently that SNRs in massive star clusters might be able to accelerate CRs up to energies of

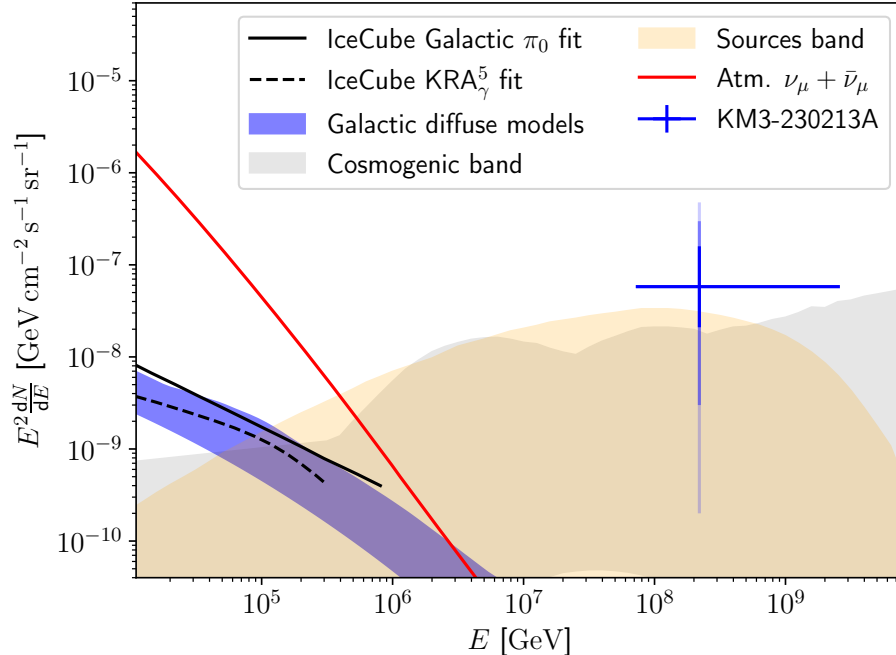


Figure 4. Expected fluxes from different models of the diffuse Galactic emission (blue band, see text for details) compared to measurements of the KM3-230213A all-sky diffuse flux from Aiello et al. (2025a) (blue data point, the different blue shades represent the 1, 2 and 3σ Feldman-Cousins confidence intervals, respectively.) IceCube measurements of the Galactic diffuse neutrino flux for different models are also shown (black lines IceCube Collaboration et al. 2023), as well as bands of the cosmogenic neutrino flux and individual extragalactic sources as in Aiello et al. (2025a). The zenith-angle averaged expected flux of atmospheric muon- and anti-muon neutrinos from Honda et al. (2007); Enberg et al. (2008) is shown in red.

hundreds of PeV (Vieu & Reville 2023). Even such an extreme scenario would only be able to produce neutrinos with energies of several tens of PeV, which is not sufficient to explain a neutrino with an energy much larger than the low end of the 90% confidence interval of KM3-230213A of 72 PeV.

We compared the positions of known SNRs from the latest version of Green’s SNR catalogue (Green 2024) with KM3-230213A (see Figure 5). No SNR close to KM3-230213A is known. Given the difficulties of accelerating CRs to the required energies and the non-detection of a SNR closeby, SNRs are very unlikely to be a potential source for KM3-230213A.

Stellar clusters: Young stellar clusters with a large number of massive stars can produce a collective wind termination shock where particles can be accelerated. Inside the Mon R2 cloud there is ongoing star formation, but to a lesser extent than in the Orion A and Orion B clouds. However, no Wolf-Rayet star was found in the region, and the most massive star is only $\sim 10 M_{\odot}$ (Rayner et al. 2017). To search for potential young stellar clusters, we use the catalogue from Celli et al. (2024). The stellar clusters are displayed in Figure 5 with magenta circles where the size of the circles corresponds to the cluster size. Two clusters are found within the KM3-230213A uncertainty region (FSR_1117 and NGC_2183), and three additional ones within 5° from the event (BDSB91, NGC_2232, and vdBergh.80). However, all of these clusters have collective wind powers $< 10^{34} \text{ erg s}^{-1}$ and therefore, there is not enough power within the collective stellar winds to allow efficient CR acceleration to the required energies (Morlino et al. 2021; Mitchell et al. 2024). Given the low wind powers, also a scenario of a SNR exploding in a massive wind-blowing cluster as in Vieu & Reville (2023) seems unlikely.

X-ray binaries and microquasars: Microquasars are a relatively new source class in the very-high-energy γ -ray regime, with SS433 being the first microquasar detected by HAWC and H.E.S.S. (Abeysekara et al. 2018; H. E. S. S. Collaboration et al. 2024). Recently, the LHAASO collaboration discovered γ -ray emission above 100 TeV from 5 sources (LHAASO Collaboration 2024). However, microquasars might lack the potential to accelerate CRs to the energies needed. In the model from Escobar et al. (2022), for example, protons reach maximum energies of only $\sim 10^{16}$ eV, which makes any potential association with KM3-230213A unlikely. X-ray binaries were searched in cata-

logues produced with eROSITA data (Neumann et al. 2023; Avakyan et al. 2023) and microquasars in the catalogue provided by Combi et al. (2008). Only a subset of X-ray binaries will also be a microquasar. As can be seen in Figure 5, no X-ray binary or microquasar is found close to KM3-230213A.

Pulsars and pulsar wind nebulae: Pulsars and pulsar wind nebulae are efficient particle accelerators and prominent sources in the γ -ray sky. A large number of LHAASO sources detected above energies of 100 TeV are potentially associated with high spin-down power pulsars. From general arguments, the maximum achievable energies in units of PeV can be written as (de Oña Wilhelmi et al. 2022)

$$E_{\max}(\text{PeV}) \approx 2\eta_e\eta_B^{1/2}\dot{E}_{36}^{1/2}, \quad (1)$$

where η_e is the ratio between the electric and magnetic field strength, η_B the fraction of the pulsar wind energy flux transferred to the magnetic field, and \dot{E}_{36} the spin-down power in units of $10^{36} \text{ erg s}^{-1}$. In ideal conditions, $\eta_e \leq 1$, and $\eta_B \leq 1$ because of energy conservation.

We searched for known pulsars in the ATNF pulsar catalogue (Manchester et al. 2005). Only two pulsars are found within a distance less than 5° from the neutrino event: B0559-05, with a distance of 4.4° , and B0621-04 with a distance of 3.8° (see Figure 5). They have spin-down powers of $8.3 \times 10^{32} \text{ erg s}^{-1}$ and $2.9 \times 10^{31} \text{ erg s}^{-1}$, respectively, which is far too low to reach even PeV energies according to Equation 1. While the situation can be different in other cases such as in binary systems (Bykov et al. 2024), the energy loss rates of the pulsars are orders of magnitude below what one might consider as a strong pulsar and are not able to accelerate CRs to the required energies. We therefore conclude that no known pulsar can be a potential CR accelerator for KM3-230213A.

If the cone of open field lines around a pulsar's magnetic pole does not point towards the Earth, no pulsed emission can be detected and a pulsar might not be recognised as such. However, a powerful pulsar is expected to produce a bright pulsar wind nebula, which could be visible in γ -rays. A large fraction of this electromagnetic radiation is believed to be of leptonic origin, but a hadronic component is not excluded. In the next section, a search for potential Galactic γ -ray sources is performed.

4. CONSTRAINTS FROM γ -RAY OBSERVATIONS

4.1. Search for potential γ -ray counterparts

Neutrino production via hadronic collisions or photo-meson production inevitably also leads to the production of γ -rays. In the very-high-energy γ -ray region, data from HAWC, LHAASO, and Fermi-LAT are available. For a Galactic source accelerating particles up to more than 100 TeV, one would expect detections in both HAWC and LHAASO, unless the γ -rays are absorbed.

Fermi-LAT, HAWC and LHAASO are survey instruments that cover the region of interest. While Fermi-LAT observes γ -ray energies from tens of MeV up to several hundreds of GeV, the HAWC and LHAASO energy ranges extend up to hundreds of TeV and even PeV energies. Because of γ -ray absorption, at energies above hundreds of TeV, HAWC and LHAASO are effectively constrained to observations within the Milky Way, whereas at Fermi-LAT energies a large number of extragalactic objects are observed. We searched for potential counterparts in the 4FGL-DR4 Fermi-LAT catalogue (Ballet et al. 2023), the 3HWC (Albert et al. 2020), and the first LHAASO catalogue (1LHAASO, Cao et al. 2024) of γ -ray sources. The 4FGL-DR4, the 3HWC, and the 1LHAASO sources plotted over the CO map of Dame et al. (2001) are shown in Figure 6. The position of KM3-230213A and the 68% and 99% containment radii are also shown.

No nearby sources from HAWC or LHAASO were found, imposing stringent constraints on any potential astrophysical sources in the region. While HAWC and LHAASO observations are much more relevant for the energy of the neutrino event, it is possible that the emission at HAWC and LHAASO energies is absorbed. This is different in the Fermi-LAT energy range, since even strong stellar ultraviolet radiation can not absorb GeV γ -rays and the electromagnetic cascades triggered by the absorption process can provide a relevant contribution to the emission at lower energies depending on the spectral shape. A source found by Fermi-LAT whose extension to higher energies is in tension with the non-detection by HAWC or LHAASO could be an absorbed Galactic source. Excluding extragalactic sources, there are two Fermi-LAT sources of unknown type within the 99% error region (Aiello et al. 2025a,b): 4FGL J0616.2-0653, and 4FGL J0624.8-0735. While 4FGL J0624.8-0735 has the potential radio source counterpart NVSS J062455-073536, of unknown type, and associated emission was detected in X-rays (Aiello et al. 2025b), no potential counterpart at other wavelengths was found for 4FGL J0616.2-0653. As argued in Aiello et al. (2025b), the source might even be extended and its γ -ray emission could potentially be explained by mismodelled diffuse emission (Aiello et al. 2025b).

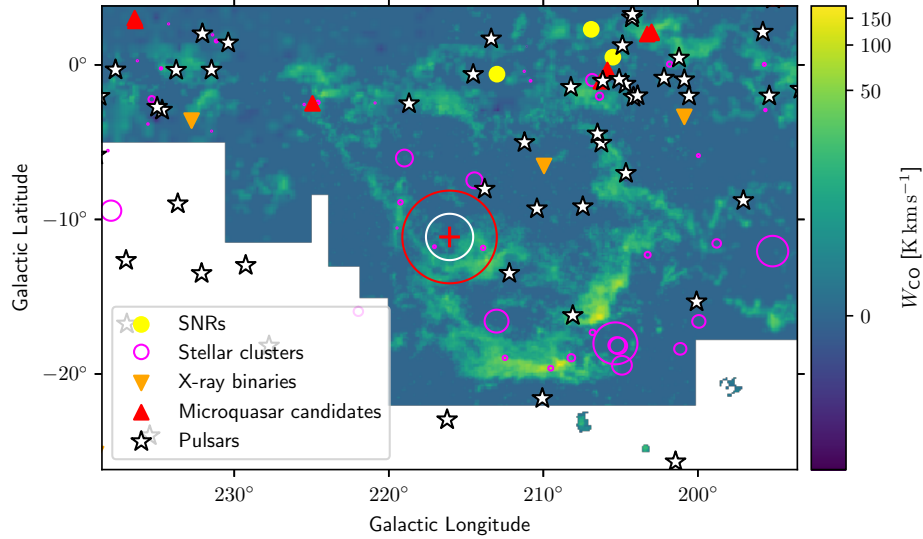


Figure 5. Different known potential CR accelerators in the region around KM3-230213A: The yellow dots represent SNRs from Green’s SNR catalogue (Green 2024), and the magenta circles show the young stellar clusters from Celli et al. (2024), the sizes of the circles correspond to the cluster sizes. X-ray binaries and microquasars are displayed with the orange and red triangles (Neumann et al. 2023; Avakyan et al. 2023), and pulsars from the ATNF pulsar catalogue (Manchester et al. 2005) as white stars with black edges. The background is the velocity-integrated CO brightness temperature from Dame et al. (2001) which traces the molecular gas.

In addition to these catalogue sources, Martí et al. (2013) performed an analysis of the source 2FGLJ0607.5-0618c, which is likely associated with the Mon R2 cloud. They reported no significant detection of γ -rays above energies of ~ 3 GeV, while at lower energies the emission is consistent with a power-law $dN/dE \propto E^{-2.73}$.

While no source in the vicinity of KM3-230213A was detected by HAWC or LHAASO, the HAWC collaboration published data accompanying the 3HWC catalogue (Albert et al. 2020). These data include skymaps with the significances and flux normalisations maximising the likelihood function¹. In this data, a point source and sources with extensions of 0.5° , 1.0° , and 2.0° are considered. The flux normalisations are given for an energy of 7 TeV by assuming a power-law of $E^{-2.5}$. Limits on the γ -ray flux, computed using the reported flux and flux error, are used to derive a limit on the neutrino emission at the KM3-230213A location.

Using the open-source *gammapy* package (Donath et al. 2023; Acero et al. 2024), we retrieved the flux and uncertainty values, corresponding to the 2σ Feldman-Cousins confidence intervals, from the skymaps. The values of the flux at 7 TeV, the corresponding upper uncertainties and the derived upper limits (the sum of flux normalisation and uncertainty) for the point source and the extended source cases are shown in Table 1. As it can be seen, the uncertainties dominate over the flux normalisations since no HAWC source is located nearby. Using these upper limits on the flux at 7 TeV and the power-law index of -2.5 , we computed the upper limits on the γ -ray flux for the whole HAWC energy range. Furthermore, the HAWC collaboration also has analysed the potential emission from nearby molecular clouds (Albert et al. 2021), amongst them Mon R2. While the cloud was not detected, upper limits were provided. These limits are also shown in the left panel of Figure 7, together with the prediction of the total emission from Mon R2 as a passive cloud from the same article.

Since an inconsistency of the extension of the γ -ray spectra observed by Fermi-LAT with the upper limits obtained from HAWC data could be explained by an absorbed source potentially emitting neutrinos at higher energies, we

¹ The data are available under <https://data.hawc-observatory.org/datasets/3hwc-survey/fitsmaps.php>

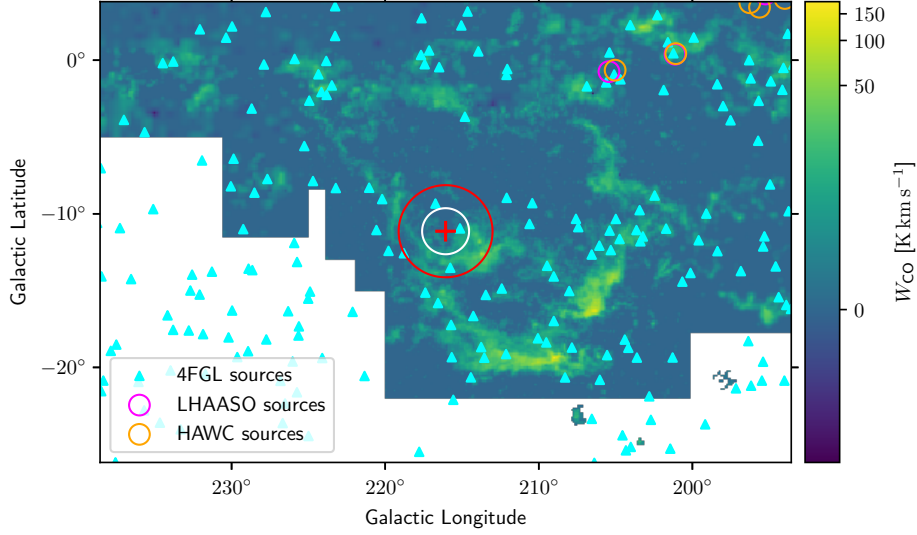


Figure 6. CO map from Dame et al. (2001) of the velocity integrated brightness temperature tracing the molecular gas as a background, KM3-230213A position (red cross) and uncertainty (white and red circles), and sources from the 4FGL-DR4 catalogue (cyan triangles, Ballet et al. 2023), the 3HWC (magenta circles, Albert et al. 2020) and the 1LHAASO catalogue (orange circles, Cao et al. 2024).

Source extension	Flux at 7 TeV [$\text{TeV}^{-1} \text{cm}^{-2} \text{s}^{-1}$]	Upper error [$\text{TeV}^{-1} \text{cm}^{-2} \text{s}^{-1}$]	Upper limit [$\text{TeV}^{-1} \text{cm}^{-2} \text{s}^{-1}$]
PS	9×10^{-18}	1.4×10^{-16}	1.5×10^{-16}
0.5°	0	2.1×10^{-16}	2.1×10^{-16}
1.0°	9×10^{-17}	4.2×10^{-16}	5.1×10^{-16}
2.0°	1.6×10^{-16}	7.5×10^{-16}	9.1×10^{-16}

Table 1. Flux normalisations from the public 3HWC data of HAWC (Albert et al. 2020) for KM3-230213A at 7 TeV with the upper error (2σ Feldman-Cousins confidence intervals) on the flux and the derived upper limits. The different rows show the point source (PS) case and the cases of extended sources with radii of 0.5° , 1.0° , and 2.0° .

compare in the left panel of Figure 7 the Fermi-LAT spectra with the HAWC limits. An extension of the Fermi-LAT spectra towards higher energies does not necessarily represent the true spectral shape of the sources. As can be seen, the measurements of Mon R2 by Fermi-LAT are consistent with the upper limits of HAWC for Mon R2 at higher energies, assuming no spectral breaks or cutoffs. Similarly, the extrapolated fluxes of 4FGL J0616.2-0653 and 4FGL J0624.8-0735 are well below the HAWC limits at the KM3-230213A position. However, the extension of the emission of Mon R2 from Fermi-LAT is below the predictions for Mon R2 at HAWC energies from Albert et al. (2021). A possible explanation for this discrepancy might be the use of the template for the Mon R2 cloud by HAWC, which was not done by Martí et al. (2013). Assuming a larger extension of the Mon R2 cloud will also yield larger γ -ray fluxes. Further uncertainties are the CR density, changes in the spectral shape and the particle density within Mon R2. Nevertheless, because the extensions of the Fermi-LAT spectra towards higher energies are consistent with the HAWC non-detection, the presence of a strong absorbed Galactic source is unlikely.

4.2. Upper limits on neutrino fluxes from HAWC non-detections

With the upper limits from HAWC, one can derive limits on the maximum possible neutrino fluxes at the energy range of KM3-230213A. While HAWC can observe sources above energies of 100 TeV (Abeysekara et al. 2020), it is not

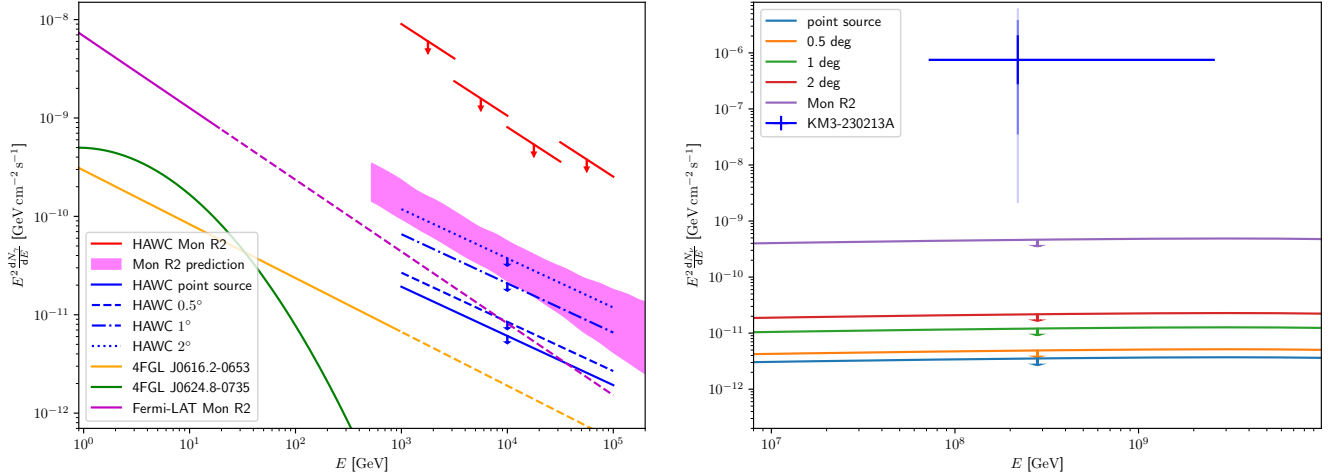


Figure 7. Left: Gamma-ray fluxes of the Fermi-LAT sources 4FGL J0616.2-0653, 4FGL J0624.8-0735, and the Fermi-LAT spectrum of Mon R2 from Martí et al. (2013) extended up to energies of 100 TeV assuming the same spectral shape as at lower energies. The 95% credible interval upper limits on Mon R2 from HAWC are shown in red (Albert et al. 2021), and the upper limits derived from public HAWC data for a point source and sources of 0.5°, 1°, and 2° extension at the position of KM3-230213A are shown in blue. The prediction of the diffuse emission from Mon R2 as a passive cloud (Albert et al. 2021) is shown with the magenta band. Right: Neutrino limits derived from the HAWC γ -ray limits shown in the left panel for a point source, extended sources of 0.5°, 1.0°, and 2.0°, and the Mon R2 cloud, assuming E^{-2} distributed CRs. The point source flux derived from the detection of KM3-230213A is shown in blue, and the different shades of colour of the flux uncertainties represent the 1 σ , 2 σ , and 3 σ Feldman-Cousins intervals.

guaranteed that the assumption of a power-law index of -2.5 is still valid at these energies and we therefore assumed that the limit only holds until 100 TeV. This is the same maximum energy for which HAWC provided upper limits for Mon R2 in Albert et al. (2021).

To obtain a limit on the neutrino flux at hundreds of PeV, we made use of the publicly available GAMERA software package (Hahn 2015; Hahn et al. 2022). We assumed a population of power-law distributed CRs producing γ -rays and neutrinos via proton-proton collisions, fulfilling the HAWC limits. The most poorly constraining neutrino limits are obtained for hard CR power-law indices. Here, we choose a power-law index of the CRs of -2 , which is the one expected in standard diffusive shock acceleration. Harder CR spectral indices are more difficult to produce, and we also note that none of the sources detected with the LHAASO Kilometer Squared Array (LHAASO KM2A, Cao et al. (2024)) has a power-law index harder than -2 . Since for hadronic collisions the γ -ray and neutrino spectra show approximately the same power-law index as the parent CRs, the existence of Galactic sources with harder CR indices than -2 above hundreds of TeV seems unlikely. For the fulfilment of the HAWC upper limits in γ -rays, this power-law index is assumed to be valid for energies above 100 TeV.

The γ -ray emission can be absorbed by the large-scale diffuse Galactic radiation fields or by radiation fields inside the source itself. To assess the impact of the large-scale Galactic radiation fields we made use of the radiation model developed by Popescu et al. (2017) together with the cosmic microwave background. At 100 TeV, even if the neutrino would have been produced at the outer edge of the Milky Way at a Galactic radius of 24 kpc (the maximum Galactic radius of the model from Popescu et al. (2017)), only 3.4% of the γ -ray emission is lost. For the Mon R2 cloud, located at a distance of 830 pc, this value reduces to 0.7%. Therefore, one can safely neglect the absorption by the large-scale fields and consider the γ -ray upper limits as a proxy for the computation of the corresponding neutrino limits.

The derived neutrino limits for a point source, sources of 0.5°, 1.0°, and 2.0° extension, and for the Mon R2 molecular cloud are shown in the right panel of Figure 7. Absorption was ignored, and it was assumed that the CRs follow an E^{-2} power-law. The fluxes reported in Aiello et al. (2025a) were derived with the assumption of an all-sky diffuse isotropic flux. Such a flux can not be directly compared with the neutrino limits for individual sources with different extensions. We therefore computed a point-source flux for KM3-230213A for the current livetime of the detector from the effective area. For the calculation of the effective area, the same selection criteria as in Aiello et al. (2025a) were applied, and for the final result we also assumed a power-law spectral shape throughout the whole energy range from

72 PeV to 2.6 EeV with a spectral index of -2 as in Aiello et al. (2025a). This flux is also displayed in the right panel of Figure 7. All neutrino limits are more than three orders of magnitude below the expected flux, and the lower 3σ uncertainty of the expected flux is still one order of magnitude above the limit of the Mon R2 cloud and two orders of magnitude or more for the other cases. Because the flux is derived from only one event, the flux derived from KM3-230213A can be considered as an upper limit to the neutrino flux. In this case, the limits derived from the HAWC data for a Galactic neutrino source are much more constraining.

An underestimation of the neutrino limits can be caused by significant absorption within the source itself. The most relevant absorbing photon energy is $(m_e c^2)^2/E_\gamma$, where $m_e c^2$ is the electron rest mass energy, and E_γ the absorbed γ -ray energy (Vernetto & Lipari 2016). For γ -ray energies of 100 TeV, the most relevant photons come from far-infrared radiation fields with energies around 3 meV. More accurate calculations with the open-source software package GAMERA yield temperature fields of 60 K, corresponding to energies of 5 meV. Strong far-infrared radiation is produced in the Galaxy when surrounding clouds reprocess the light from massive stellar clusters. For non-ionizing ultraviolet radiation fields with energy densities of several hundreds of eV cm^{-3} , one can produce far-infrared energy densities up to 100 eV cm^{-3} (Dopita et al. 2005; Groves et al. 2008; Popescu et al. 2011). However, for a 60 K radiation field with an energy density of 100 eV cm^{-3} , the attenuation length is $\sim 400 \text{ pc}$, which is much larger than the size of the whole Mon R2 cloud. It is therefore highly unlikely, that a strong hidden Galactic source producing large neutrino fluxes at the required energies exists.

5. CONCLUSION

In this article, we explored the possibility that the highest energy candidate neutrino event ever detected KM3-230213A could be produced within our own Galaxy. We searched for potential gas targets and found, that the Monoceros R2 cloud is within the 99% containment radius and could serve as a target for accelerated particles. However, the diffuse Galactic emission is insufficient to produce such an event flux. A search for potential γ -ray counterparts revealed two unidentified Fermi-LAT sources, but no detection by HAWC and LHAASO. Using publicly available HAWC data, we derived upper limits on the γ -ray and potential neutrino emission. The limits derived from HAWC data on potential Galactic neutrino emission are orders of magnitude below the flux calculated from KM3-230213A when interpreted as a point-source flux. The only hypothetical exception could be an absorbed γ -ray source with a very hard spectrum. However, nearly all conceivable Galactic CR accelerators struggle with producing the required maximum energies and no counterpart can be found in the region. We conclude that it is very unlikely that the event originated from within the Milky Way. Therefore, an extragalactic origin is much more likely.

ACKNOWLEDGEMENTS

The authors acknowledge the financial support of: KM3NeT-INFRADEV2 project, funded by the European Union Horizon Europe Research and Innovation Programme under grant agreement No 101079679; Funds for Scientific Research (FRS-FNRS), Francqui foundation, BAEF foundation. Czech Science Foundation (GAČR 24-12702S); Agence Nationale de la Recherche (contract ANR-15-CE31-0020), Centre National de la Recherche Scientifique (CNRS), Commission Européenne (FEDER fund and Marie Curie Program), LabEx UnivEarthS (ANR-10-LABX-0023 and ANR-18-IDEX-0001), Paris Île-de-France Region, Normandy Region (Alpha, Blue-waves and Neptune), France, The Provence-Alpes-Côte d’Azur Delegation for Research and Innovation (DRARI), the Provence-Alpes-Côte d’Azur region, the Bouches-du-Rhône Departmental Council, the Metropolis of Aix-Marseille Provence and the City of Marseille through the CPER 2021-2027 NEUMED project, The CNRS Institut National de Physique Nucléaire et de Physique des Particules (IN2P3); Shota Rustaveli National Science Foundation of Georgia (SRNSFG, FR-22-13708), Georgia; This work is part of the MuSES project which has received funding from the European Research Council (ERC) under the European Union’s Horizon 2020 Research and Innovation Programme (grant agreement No 101142396); The General Secretariat of Research and Innovation (GSRI), Greece; Istituto Nazionale di Fisica Nucleare (INFN) and Ministero dell’Università e della Ricerca (MUR), through PRIN 2022 program (Grant PANTHEON 2022E2J4RK, Next Generation EU) and PON R&I program (Avviso n. 424 del 28 febbraio 2018, Progetto PACK-PIR01 00021), Italy; IDMAR project Po-Fesr Sicilian Region az. 1.5.1; A. De Benedittis, W. Idrissi Ibsalikh, M. Bendahman, A. Nayerhoda, G. Papalashvili, I. C. Rea, A. Simonelli have been supported by the Italian Ministero dell’Università e della Ricerca (MUR), Progetto CIR01 00021 (Avviso n. 2595 del 24 dicembre 2019); KM3NeT4RR MUR Project National Recovery and Resilience Plan (NRRP), Mission 4 Component 2 Investment 3.1, Funded by the European Union – NextGenerationEU, CUP I57G21000040001, Concession Decree MUR No. n. Prot. 123 del 21/06/2022;

Ministry of Higher Education, Scientific Research and Innovation, Morocco, and the Arab Fund for Economic and Social Development, Kuwait; Nederlandse organisatie voor Wetenschappelijk Onderzoek (NWO), the Netherlands; The grant “AstroCeNT: Particle Astrophysics Science and Technology Centre”, carried out within the International Research Agendas programme of the Foundation for Polish Science financed by the European Union under the European Regional Development Fund; The program: “Excellence initiative-research university” for the AGH University in Krakow; The ARTIQ project: UMO-2021/01/2/ST6/00004 and ARTIQ/0004/2021; Ministry of Research, Innovation and Digitalisation, Romania; Slovak Research and Development Agency under Contract No. APVV-22-0413; Ministry of Education, Research, Development and Youth of the Slovak Republic; MCIN for PID2021-124591NB-C41, -C42, -C43 and PDC2023-145913-I00 funded by MCIN/AEI/10.13039/501100011033 and by “ERDF A way of making Europe”, for ASFAE/2022/014 and ASFAE/2022 /023 with funding from the EU NextGenerationEU (PRTR-C17.I01) and Generalitat Valenciana, for Grant AST22.6.2 with funding from Consejería de Universidad, Investigación e Innovación and Gobierno de España and European Union - NextGenerationEU, for CSIC-INFRA23013 and for CNS2023-144099, Generalitat Valenciana for CIDEAGENT/2018/034, /2019/043, /2020/049, /2021/23, for CIDEIG/2023/20, for CIPROM/2023/51 and for GRISOLIAP/2021/192 and EU for MSC/101025085, Spain; Khalifa University internal grants (ESIG-2023-008, RIG-2023-070 and RIG-2024-047), United Arab Emirates; The European Union’s Horizon 2020 Research and Innovation Programme (ChETEC-INFRA - Project no. 101008324).

REFERENCES

- Aartsen, M. G., Abraham, K., Ackermann, M., et al. 2016, *ApJ*, 833, 3, doi: [10.3847/0004-637X/833/1/3](https://doi.org/10.3847/0004-637X/833/1/3)
- Abbasi, R., Ackermann, M., Adams, J., et al. 2024, *PhRvD*, 110, 022001, doi: [10.1103/PhysRevD.110.022001](https://doi.org/10.1103/PhysRevD.110.022001)
- Abdul Halim, A., Abreu, P., Aglietta, M., et al. 2024, *ApJ*, 976, 48, doi: [10.3847/1538-4357/ad843b](https://doi.org/10.3847/1538-4357/ad843b)
- Abeysekara, A. U., Albert, A., Alfaro, R., et al. 2018, *Nature*, 562, 82, doi: [10.1038/s41586-018-0565-5](https://doi.org/10.1038/s41586-018-0565-5)
- . 2020, *PhRvL*, 124, 021102, doi: [10.1103/PhysRevLett.124.021102](https://doi.org/10.1103/PhysRevLett.124.021102)
- Acero, F., Bernete, J., Biederbeck, N., et al. 2024, *Gammapy: Python toolbox for gamma-ray astronomy*, v1.2, Zenodo, doi: [10.5281/zenodo.10726484](https://doi.org/10.5281/zenodo.10726484)
- Aiello, S., et al. 2025a, *Nature*, doi: [10.1038/s41586-024-08543-1](https://doi.org/10.1038/s41586-024-08543-1)
- . 2025b, submitted to *arXiv*
- Albert, A., André, M., Anghinolfi, M., et al. 2018, *ApJL*, 853, L7, doi: [10.3847/2041-8213/aaa4f6](https://doi.org/10.3847/2041-8213/aaa4f6)
- Albert, A., Alfaro, R., Alvarez, C., et al. 2020, *ApJ*, 905, 76, doi: [10.3847/1538-4357/abc2d8](https://doi.org/10.3847/1538-4357/abc2d8)
- . 2021, *ApJ*, 914, 106, doi: [10.3847/1538-4357/abfc47](https://doi.org/10.3847/1538-4357/abfc47)
- Albert, A., Alves, S., André, M., et al. 2024, *JCAP*, 2024, 038, doi: [10.1088/1475-7516/2024/08/038](https://doi.org/10.1088/1475-7516/2024/08/038)
- Allakhverdyan, V. A., Avrorin, A. D., Avrorin, A. V., et al. 2023, *PhRvD*, 107, 042005, doi: [10.1103/PhysRevD.107.042005](https://doi.org/10.1103/PhysRevD.107.042005)
- Amenomori, M., Bao, Y. W., Bi, X. J., et al. 2021, *PhRvL*, 126, 141101, doi: [10.1103/PhysRevLett.126.141101](https://doi.org/10.1103/PhysRevLett.126.141101)
- Avakyan, A., Neumann, M., Zainab, A., et al. 2023, *A&A*, 675, A199, doi: [10.1051/0004-6361/202346522](https://doi.org/10.1051/0004-6361/202346522)
- Ballet, J., Bruel, P., Burnett, T. H., Lott, B., & The Fermi-LAT collaboration. 2023, *arXiv e-prints*, arXiv:2307.12546, doi: [10.48550/arXiv.2307.12546](https://doi.org/10.48550/arXiv.2307.12546)
- Bartoli, B., Bernardini, P., Bi, X. J., et al. 2015, *ApJ*, 806, 20, doi: [10.1088/0004-637X/806/1/20](https://doi.org/10.1088/0004-637X/806/1/20)
- Bell, A. R., Schure, K. M., Reville, B., & Giacinti, G. 2013, *MNRAS*, 431, 415, doi: [10.1093/mnras/stt179](https://doi.org/10.1093/mnras/stt179)
- Breuhaus, M., Hinton, J. A., Joshi, V., Reville, B., & Schoorlemmer, H. 2022, *A&A*, 661, A72, doi: [10.1051/0004-6361/202141318](https://doi.org/10.1051/0004-6361/202141318)
- Bykov, A. M., Petrov, A. E., Ponomaryov, G. A., Levenfish, K. P., & Falanga, M. 2024, *Advances in Space Research*, 74, 4276, doi: [10.1016/j.asr.2024.01.021](https://doi.org/10.1016/j.asr.2024.01.021)
- Cao, Z., Aharonian, F., An, Q., et al. 2023, *PhRvL*, 131, 151001, doi: [10.1103/PhysRevLett.131.151001](https://doi.org/10.1103/PhysRevLett.131.151001)
- . 2024, *ApJS*, 271, 25, doi: [10.3847/1538-4365/acfd29](https://doi.org/10.3847/1538-4365/acfd29)
- Carpenter, J. M., & Hodapp, K. W. 2008, in *Handbook of Star Forming Regions*, Volume I, ed. B. Reipurth, Vol. 4, 899, doi: [10.48550/arXiv.0809.1396](https://doi.org/10.48550/arXiv.0809.1396)
- Celli, S., Specovius, A., Menchiari, S., Mitchell, A., & Morlino, G. 2024, *A&A*, 686, A118, doi: [10.1051/0004-6361/202348541](https://doi.org/10.1051/0004-6361/202348541)
- Combi, J. A., Albacete-Colombo, J. F., & Martí, J. 2008, *A&A*, 477, 125, doi: [10.1051/0004-6361:20078292](https://doi.org/10.1051/0004-6361:20078292)
- Dame, T. M., Hartmann, D., & Thaddeus, P. 2001, *ApJ*, 547, 792, doi: [10.1086/318388](https://doi.org/10.1086/318388)
- De La Torre Luque, P., Gaggero, D., Grasso, D., & Marinelli, A. 2022, *Frontiers in Astronomy and Space Sciences*, 9, 1041838, doi: [10.3389/fspas.2022.1041838](https://doi.org/10.3389/fspas.2022.1041838)
- de Oña Wilhelmi, E., López-Coto, R., Amato, E., & Aharonian, F. 2022, *ApJL*, 930, L2, doi: [10.3847/2041-8213/ac66cf](https://doi.org/10.3847/2041-8213/ac66cf)

- Donath, A., Terrier, R., Remy, Q., et al. 2023, *A&A*, 678, A157, doi: [10.1051/0004-6361/202346488](https://doi.org/10.1051/0004-6361/202346488)
- Dopita, M. A., Groves, B. A., Fischera, J., et al. 2005, *ApJ*, 619, 755, doi: [10.1086/423948](https://doi.org/10.1086/423948)
- Enberg, R., Reno, M. H., & Sarcevic, I. 2008, *PhRvD*, 78, 043005, doi: [10.1103/PhysRevD.78.043005](https://doi.org/10.1103/PhysRevD.78.043005)
- Escobar, G. J., Pellizza, L. J., & Romero, G. E. 2022, *A&A*, 665, A145, doi: [10.1051/0004-6361/202142753](https://doi.org/10.1051/0004-6361/202142753)
- Ferrière, K. 1998, *ApJ*, 497, 759, doi: [10.1086/305469](https://doi.org/10.1086/305469)
- Ferrière, K., Gillard, W., & Jean, P. 2007, *A&A*, 467, 611, doi: [10.1051/0004-6361:20066992](https://doi.org/10.1051/0004-6361:20066992)
- Gaggero, D., Grasso, D., Marinelli, A., Urbano, A., & Valli, M. 2015, *ApJL*, 815, L25, doi: [10.1088/2041-8205/815/2/L25](https://doi.org/10.1088/2041-8205/815/2/L25)
- Green, D. A. 2024, arXiv e-prints, arXiv:2411.03367, doi: [10.48550/arXiv.2411.03367](https://doi.org/10.48550/arXiv.2411.03367)
- Groves, B., Dopita, M. A., Sutherland, R. S., et al. 2008, *ApJS*, 176, 438, doi: [10.1086/528711](https://doi.org/10.1086/528711)
- H. E. S. S. Collaboration, Aharonian, F., Ait Benkhali, F., et al. 2024, *Science*, 383, 402, doi: [10.1126/science.adi2048](https://doi.org/10.1126/science.adi2048)
- Hahn, J. 2015, in *International Cosmic Ray Conference*, Vol. 34, 34th International Cosmic Ray Conference (ICRC2015), 917, doi: [10.22323/1.236.0917](https://doi.org/10.22323/1.236.0917)
- Hahn, J., Romoli, C., & Breuhaus, M. 2022, *GAMERA: Source modeling in gamma astronomy*, *Astrophysics Source Code Library*, record ascl:2203.007
- Herbst, W., & Racine, R. 1976, *AJ*, 81, 840, doi: [10.1086/111963](https://doi.org/10.1086/111963)
- Honda, M., Kajita, T., Kasahara, K., Midorikawa, S., & Sanuki, T. 2007, *PhRvD*, 75, 043006, doi: [10.1103/PhysRevD.75.043006](https://doi.org/10.1103/PhysRevD.75.043006)
- Hörandel, J. R. 2003, *Astroparticle Physics*, 19, 193, doi: [10.1016/S0927-6505\(02\)00198-6](https://doi.org/10.1016/S0927-6505(02)00198-6)
- IceCube Collaboration. 2013, *Science*, 342, 1242856, doi: [10.1126/science.1242856](https://doi.org/10.1126/science.1242856)
- IceCube Collaboration, Aartsen, M. G., Ackermann, M., et al. 2018, *Science*, 361, eaat1378, doi: [10.1126/science.aat1378](https://doi.org/10.1126/science.aat1378)
- IceCube Collaboration, Abbasi, R., Ackermann, M., et al. 2022, *Science*, 378, 538, doi: [10.1126/science.abg3395](https://doi.org/10.1126/science.abg3395)
- . 2023, *Science*, 380, 1338, doi: [10.1126/science.adc9818](https://doi.org/10.1126/science.adc9818)
- Jiang, S. D., & Hillenbrand, L. A. 2024, *AJ*, 167, 221, doi: [10.3847/1538-3881/ad2fb0](https://doi.org/10.3847/1538-3881/ad2fb0)
- Lagage, P. O., & Cesarsky, C. J. 1983, *A&A*, 125, 249
- LHAASO Collaboration. 2024, arXiv e-prints, arXiv:2410.08988, doi: [10.48550/arXiv.2410.08988](https://doi.org/10.48550/arXiv.2410.08988)
- Maddalena, R. J., Morris, M., Moskowitz, J., & Thaddeus, P. 1986, *ApJ*, 303, 375, doi: [10.1086/164083](https://doi.org/10.1086/164083)
- Manchester, R. N., Hobbs, G. B., Teoh, A., & Hobbs, M. 2005, *AJ*, 129, 1993, doi: [10.1086/428488](https://doi.org/10.1086/428488)
- Marcowith, A., Dwarkadas, V. V., Renaud, M., Tatischeff, V., & Giacinti, G. 2018, *MNRAS*, 479, 4470, doi: [10.1093/mnras/sty1743](https://doi.org/10.1093/mnras/sty1743)
- Martí, J., Luque-Escamilla, P. L., Muñoz-Arjonilla, A. J., et al. 2013, *A&A*, 556, A131, doi: [10.1051/0004-6361/201220791](https://doi.org/10.1051/0004-6361/201220791)
- Mitchell, A. M. W., Morlino, G., Celli, S., Menchiari, S., & Specovius, A. 2024, arXiv e-prints, arXiv:2403.16650, doi: [10.48550/arXiv.2403.16650](https://doi.org/10.48550/arXiv.2403.16650)
- Morlino, G., Blasi, P., Peretti, E., & Cristofari, P. 2021, *MNRAS*, 504, 6096, doi: [10.1093/mnras/stab690](https://doi.org/10.1093/mnras/stab690)
- Neininger, N., Guélin, M., Ungerechts, H., Lucas, R., & Wielebinski, R. 1998, *Nature*, 395, 871, doi: [10.1038/27612](https://doi.org/10.1038/27612)
- Neumann, M., Avakyan, A., Doroshenko, V., & Santangelo, A. 2023, *A&A*, 677, A134, doi: [10.1051/0004-6361/202245728](https://doi.org/10.1051/0004-6361/202245728)
- Popescu, C. C., Tuffs, R. J., Dopita, M. A., et al. 2011, *A&A*, 527, A109, doi: [10.1051/0004-6361/201015217](https://doi.org/10.1051/0004-6361/201015217)
- Popescu, C. C., Yang, R., Tuffs, R. J., et al. 2017, *MNRAS*, 470, 2539, doi: [10.1093/mnras/stx1282](https://doi.org/10.1093/mnras/stx1282)
- Racine, R. 1968, *AJ*, 73, 233, doi: [10.1086/110624](https://doi.org/10.1086/110624)
- Rayner, T. S. M., Griffin, M. J., Schneider, N., et al. 2017, *A&A*, 607, A22, doi: [10.1051/0004-6361/201630039](https://doi.org/10.1051/0004-6361/201630039)
- Schlafly, E. F., Green, G., Finkbeiner, D. P., et al. 2014, *ApJ*, 786, 29, doi: [10.1088/0004-637X/786/1/29](https://doi.org/10.1088/0004-637X/786/1/29)
- Vernetto, S., & Lipari, P. 2016, *PhRvD*, 94, 063009, doi: [10.1103/PhysRevD.94.063009](https://doi.org/10.1103/PhysRevD.94.063009)
- Vieu, T., & Reville, B. 2023, *MNRAS*, 519, 136, doi: [10.1093/mnras/stac3469](https://doi.org/10.1093/mnras/stac3469)